

---

# Inertial Confinement Fusion Forecasting via LLMs

---

**Mingkai Chen**  
Rochester Institute of Technology  
mxceec@rit.edu

**Taowen Wang**  
Rochester Institute of Technology  
tw9146@rit.edu

**James Chenhao Liang**  
Rochester Institute of Technology  
jcl3689@rit.edu

**Chuan Liu**  
University of Rochester  
cliu81@ur.rochester.edu

**Chunshu Wu**  
University of Rochester  
cwu88@ur.rochester.edu

**Qifan Wang**  
Meta AI  
wqfcr@meta.com

**Ying Nian Wu**  
University of California, Los Angeles  
ywu@stat.ucla.edu

**Michael Huang**  
University of Rochester  
michael.huang@rochester.edu

**Chuang Ren**  
University of Rochester  
chuang.ren@rochester.edu

**Ang Li**  
Pacific Northwest National Laboratory  
ang.li@pnl.gov

**Tong Geng**  
University of Rochester  
tong.geng@rochester.edu

**Dongfang Liu\***  
Rochester Institute of Technology  
dongfang.liu@rit.edu

## Abstract

Controlled fusion energy is deemed pivotal for the advancement of human civilization. In this study, we introduce **FUSION-LLM**, a novel integration of Large Language Models (LLMs) with classical reservoir computing paradigms tailored to address challenges in Inertial Confinement Fusion (ICF). Our approach offers several key contributions: Firstly, we propose the *LLM-anchored Reservoir*, augmented with a fusion-specific prompt, enabling accurate forecasting of hot electron dynamics during implosion. Secondly, we develop *Signal-Digesting Channels* to temporally and spatially describe the laser intensity across time, capturing the unique characteristics of ICF inputs. Lastly, we design the *Confidence Scanner* to quantify the confidence level in forecasting, providing valuable insights for domain experts to design the ICF process. Extensive experiments demonstrate the superior performance of our method, achieving 1.90 CAE, 0.14 top-1 MAE, and 0.11 top-5 MAE in predicting Hard X-ray (HXR) energies of ICF tasks, which presents state-of-the-art comparisons against concurrent best systems. Additionally, we present FUSION4AI, the first ICF benchmark based on physical experiments, aimed at fostering novel ideas in plasma physics research and enhancing the utility of LLMs in scientific exploration. Overall, our work strives to forge an innovative synergy between AI and plasma science for advancing fusion energy.

---

\*Corresponding author.

# 1 Introduction

“...human society remains at a Type 0, a primitive form of civilization...”

– The Kardashev scale [34]

After National Ignition Facility (NIF) achieving ignition in December 2022 [1], the focus of current inertial confinement fusion (ICF) research shifts to exploring high gain schemes required to make fusion a practical and sustainable energy source for humankind. Fusion represents a potential key enabler for advancing humanity towards a Type I civilization on the Kardashev scale [91], offering a virtually limitless and clean energy source that could power our civilization globally. This advancement could potentially resolve numerous crises we currently face — *e.g.*, economic recessions and climate change — by eliminating the need for finite resources like fossil fuels.

The optimization of ICF designs and the achievement of reliable ignition face formidable constraints [8, 14] due to laser-plasma instabilities (LPI)[22, 54]. Efficient and symmetrical driving of the target, vital for ICF, is impeded by LPI phenomena such as stimulated Raman and Brillouin backscatterings (SRS and SBS), which can disrupt implosion symmetry and reduce efficiency through cross-beam energy transfer (CBET) [68, 21]. Hot electrons, a byproduct of LPI processes like SRS and Two-Plasmon-Decay (TPD), can both hinder and assist ignition, showcasing the complexity of the interaction. Despite efforts to measure and simulate hot electrons, obtaining predictive scaling laws remains challenging due to the dynamic nature of laser/plasma conditions and computational limitations [38, 57, 89, 66, 42], highlighting the current gap in establishing a predictive capability based on first principles that aligns with experimental data. These constraints highlight the need for an innovative approach to overcome these obstacles.

Currently, Large Language Models (LLMs) exhibit versatile capabilities across diverse disciplines (*e.g.*, robotics [44, 73, 90, 26], medical health [41, 67, 77, 50], agriculture [56, 80]), adeptly capturing intricate patterns in multimodal data. Due to their success in other domains [39, 93, 46], we are convinced that LLMs may also potentially excel in generalizing to plasma physics, particularly in forecasting the behavior of hot electrons generated during implosion in the real-world, physics experiments. Leveraging their vast pre-trained knowledge base, LLMs could optimize ICF designs by efficiently evaluating numerous scenarios, aiding researchers in identifying promising approaches expediently, and generating insights to enhance our understanding and control of the fusion process.

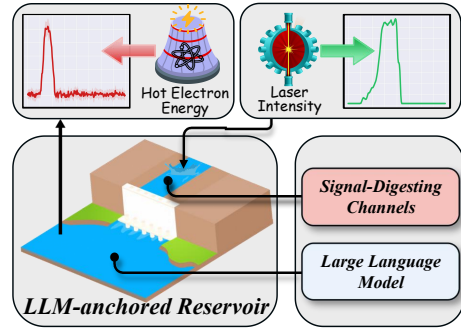


Figure 1: The overview of **FUSION-LLM**.

In light of this perspective, we intend to harness the power of LLMs to overcome the barrier to the vertical advancement of the next stage of human civilization: fusion energy. This science problem manifests as two sub-problems in a unique and challenging setup: ❶ how to *tailor pre-trained LLMs* in order to accurately predict the behavior of hot electrons based on laser intensity inputs? and ❷ how to evaluate the *trustworthiness* of the LLM’s predictions in order to guide the ICF design?

We conceptualize LLMs as a computational reservoir to unlock their potential for robust domain adaptation and generalization for ICF task, titled **FUSION-LLM** (see Fig. 1). In order to address question ❶, we propose the *LLM-anchored Reservoir*, augmented with a fusion-specific prompt, to facilitate the interpretation of plasma physics. The incorporated prompts encompass domain-specific knowledge, instructional cues, and statistical information, thereby enabling the LLMs to accommodate the specific demands of the given task. Additionally, we develop the *Signal-Digesting Channels* to capture the distinctive characteristics of ICF inputs. It features a temporal encoder to better align the laser signals with the pre-trained, time-series space, and a spatial encoder to provide a global description of the input landscape. To tackle question ❷, we introduce the *Confidence Scanner* to assess the trustworthiness in predictions. Specifically, we couple the gradient saliency in prediction head and token entropy in LLM outputs to obtain the model’s confidence scores.

Overall, this study aims to provide an exciting synergy between the domain of AI and plasma science for fusion energy development. The core contributions of this paper can be summarized as follows:

- We represent a **pioneer investigation** into the use of LLMs for analyzing hot electron dynamics in ICF. LLMs offer a cost-effective alternative compared to both plasma-physics experiments and simulations at the ignition scale. Empirical evidence (see §3/S2) showcases the efficacy of the application of LLM for plasma physics study, which directly benefits the practical design of ICF.
- We construct an **LLM-anchored reservoir computing** framework to predict the hot electron dynamics in ICF implosions. Compared to prior arts in reservoir computing [43, 20] and time-series-based LLM [31], our approach requires less data (see Table 2d) and shorter training schedule (see Table 2e), while achieving superior performance.
- We develop the **first fusion benchmark** — FUSION4AI (see §3.1) based on physical experiments, to facilitate new ideas in plasma physics research and the use of LLMs in scientific exploration.

## 2 Methodology

### 2.1 Preliminary

**The ICF Overview.** A ICF shot is depicted in Fig. 2. Laser beams  are directed towards a target fuel pellet , rapidly heating its surface to generate a plasma envelope . This plasma envelope subsequently undergoes implosion through a rocket-like expulsion of material, compressing the pellet to densities exceeding that of lead by twenty-fold and attaining ignition temperatures of approximately 100,000,000°C, thus initiating fusion reactions. Throughout this process, laser-induced plasma instabilities give rise to hot electrons, which may prematurely heat the pellet and emit Hard X-Rays (HXR) emissions  as they interact within the plasma environment. Understanding the hot electron dynamics is crucial for guiding the design of the ICF. In the context, HXR diagnostics have been extensively applied in studies at facilities such as OMEGA [69, 88, 71, 87] and the NIF [58, 59, 70]. It is however worth noting that conducting these experiments is extremely expensive (around **\$1m for one shot**).

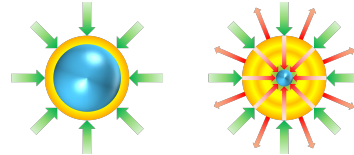


Figure 2: The ICF pipeline.

**Experiment and Data Collection.** To collect the fusion data, we conduct 100 real-world shots of ICF. Each shot is accompanied by detailed configurations including the size of the fuel pellet, the phase plate of the laser, and the input laser profile. We also measure raw sensor readings regarding HXR, which can be further converted into charges of hot electrons, allowing for the subsequent calculation of the total energy of these electrons based on their temperature. In this study, we focus on forecasting the energy from HXR emissions by given laser intensity inputs throughout the shot. This data is indispensable for physicists to ascertain and analyze the state of ICF.

### 2.2 FUSION-LLM

In this section, we introduce FUSION-LLM, a novel approach for predicting LPI and hot-electron generation in ICF. Illustrated in Fig. 3, the inputs comprise fusion-specific prompts and the time series of input laser intensity, which are processed through LLM for feature extraction. Subsequently, the output module makes predictions of hot-electron energy along with confidence scores. Our approach is characterized by three core modules: *LLM-anchored Reservoir*, which establishes a reservoir foundation using LLMs to comprehend the dynamic impact of laser intensity on hot-electron energy emission; *Signal-Digesting Channels* is responsible for encoding the time series of input laser intensity, capturing the temporal characteristics of sequential details, and spatial distinctiveness of data landscapes; and *Confidence Scanner*, tasked with estimating prediction confidence for each shot, thereby providing trustworthy guidance for practical experimental design of the ICF.

#### 2.2.1 LLM-anchored Reservoir

In classic reservoir computing (RC), a fixed, randomly generated reservoir (*e.g.*, RNN) transforms input data into a high-dimensional representation. A trainable output layer then maps this representation to the desired output. RC has gained popularity in the scientific community due to its ability to enable efficient processing of sequential data with simple training methods. Following the RC convention, we construct a reservoir using LLM with a shallow prediction head (see §S1). Due to the extensive pre-training, LLMs are equipped with robust generalization capabilities for in-context reasoning and time-series forecasting. To leverage the physics knowledge embedded in LLMs, we design *fusion-specific prompts* (FSP) that strategically connect the LLM’s vast knowledge base to the

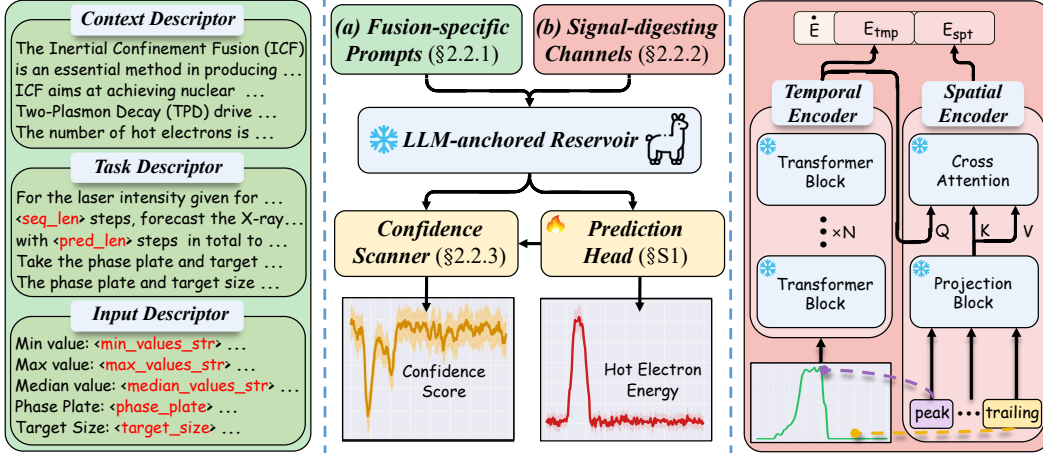


Figure 3: **FUSION-LLM framework.** (a) *Fusion-specific prompts* structure domain textual prompts with context, task and input descriptions (see §2.2.1 for details). (b) *Signal-digesting channels* comprise a pre-trained temporal encoder to extract time-series features of laser signals, and a spatial encoder to encode critical landscapes of the inputs (see §2.2.2 for details). For simplicity, we skip some architectural modules. We provide implementation details in appendix (see §S1).

specific nuances of the ICF domain. Our LLM-anchored reservoir can be defined by:

$$s[t + 1] = f(s[t], E_{las}, **\text{Prompt}), \quad (1)$$

where  $s[t]$  denotes the state of the reservoir at time step  $t$  and  $E_{las}$  represents input laser intensity.

The **\*\*Prompt** specifically denotes the structured FSP, comprising three descriptors (see Fig. 3a) designed with particular focus: **► Context descriptor** provides a detailed overview of the ICF process, highlighting the nature, sources, and characteristics of the data. It elaborates on the experimental procedures (see §2.1) used in data collection, emphasizing principles and methodologies specific to ICF. This descriptor enhances the LLMs’ comprehension of the experimental context. **► Task descriptor** outlines explicit instructions for the prediction tasks, including the format and expected length of the output. It guides the inference and forecasting process by specifying imperative considerations, ensuring that the forecasting align with domain-specific insights. **► Input descriptor** presents a concise statistical summary of the input data, offering insights into its distribution and key characteristics such as minimum, maximum, and median values. This descriptor is vital for informing the LLMs about the underlying statistical properties of the input signals. Collectively, this prompting strategy facilitates the LLMs’ ability to mine intricate input signals and produce predictions that are scientifically robust and contextually coherent within the phase space of the reservoir.

In general, our LLM-based design expands the applications and capabilities of reservoir computing, offering two significant advantages in leveraging artificial intelligence for scientific exploration:

- *Adaptability for science.* The utilization of LLMs in ICF forecasting exhibits notable adaptability in confronting the pivotal scientific challenge – modeling LPI and hot electron generation. Later, we will present empirical evidence to substantiate the systemic efficacy (see §3.1). The success of this methodology is poised to provide a generic alternative for other adjacent scientific domains in pursuit of LLM-based solutions.
- *Efficiency for data scarcity.* Gratitude is extended for the extensive pre-trained knowledge base and the precise delineation of prompt descriptors. Leveraging these assets, the LLM-based system mitigates data dependency to the  $K$ -shot level — 80 shots in our experiments — exemplifying the advantageous efficiency in addressing the persistent challenge of data scarcity in scientific inquiry.

## 2.2.2 Signal-Digesting Channels

With the establishment of the LLM-based approach described in §2.2.1, robust predictions can be immediately attained (see Table 2c). Due to the uniqueness of the ICF data, the input HXR signal exhibits its time-series, temporal landscape. Recognizing the sensitivity of LLMs to input data [64, 65], we introduce *Signal-Digesting Channels* (SDC), conceptually aligned with our reservoir design, to capture crucial input characteristics and further augment the performance of LLMs.

For the ICF process, the hot electron energy emitted during the initial and terminal phases is characterized by relatively uniform values, in contrast to the target impact phase, where peak values are observed. This laser intensity signal landscape exhibits significant discrepancies between the uniformity of the plain phase and the peaks of the impact phase. This physics insight guides our design (see Fig. 3b), which comprises two components: a *temporal encoder* to align the laser intensities with the pre-trained time-series space, and a *spatial encoder* to delineate the landscape of input data.

► *Temporal encoder* is designed to extract time-series features using a windowing mechanism that constructs consistent signal patches across sequential time steps. It employs a set of Transformer layers [85] to capture time-series distributions over the forecast horizon. This process is formulated as  $f_{tmp} : (X_{t-l:t+h}, Y_{t-l:t}) \mapsto \hat{\psi}$ , where  $X$  and  $Y$  represent the input data and target data spanning time windows of length  $l$  and  $h$  at time  $t$ . The encoder is pre-trained on a large-scale time-series dataset (see §S1 for details) and is optimized using the log-likelihood of the forecast:

$$\arg \max_{\theta} \mathbb{E}_{(X,Y) \sim p(D)} \log p(Y_{t:t+h} | f_{tmp}(X_{t-l:t+h}, Y_{t-l:t})),$$

where  $p(D)$  represents the data distribution from which the time-series samples are drawn. During fine-tuning on the target-domain ICF data, all pre-trained parameters are frozen, except for the last linear layer. The temporal encoder is utilized for feature extraction over the input laser signals  $I$ , producing temporal tokens denoted as  $E_{tmp} = f_{tmp}(I)$  for subsequent processing.

► *Spatial encoder* is designed to analyze the input signals by providing a qualitative overview of the input landscape. Specifically, it is structured to characterize the spatial patterns of laser intensity signals throughout the ICF process. We utilize the projection block  $f_{LLM}$  to project sets of critical contexts into spatial features, denoted as  $E_{spt} = \{f_{LLM}(\text{“pulse”}), f_{LLM}(\text{“peak”}), \dots, f_{LLM}(\text{“trailing”})\}$ . In practice,  $E_{spt}$  is further processed by a cross-attention layer with temporal features  $E_{tmp}$ . This step couples the contextual description to the actual signal distribution within the ICF, enabling the LLM to better capture the observed physical phenomena for predictions.

After acquiring the features from both the temporal and spatial encoders, we concatenate them  $\hat{E} = [E_{tmp}; E_{spt}]$  to form the output of DSC. Here, we use  $\hat{E}$  as augmented inputs to replace the vanilla  $E_{las}$  in Eq.1. Fundamentally, DSC introduces a novel method for input encoding in reservoir computing, which enhances overall system performance. This design offers the following advantages:

- *Discernment for temporal pattern.* With the pre-trained temporal encoder, SDC adeptly captures crucial time-series features of laser signals that correlate with HXR outputs. This merit enables the LLM to recognize distinct patterns across various time steps, representing an improvement over strong reservoir models (see Table 2c), which struggle to manage ICF’s temporal patterns.
- *In-context reasoning in signal processing.* SDC tackles the complexity of processing signals with diverse attributes, such as those found in the uniform and peak phases within ICF. Through the integration of contextual disciplinary knowledge, SDC, equipped with in-context reasoning, significantly boosts the effectiveness of LLM backbone (see Table 2c). This enhancement enables robust performance even in the face of inherent fluctuations (*i.e.*, uniform *vs.* peak in ICF).

### 2.2.3 Confidence Scanner

Trustworthiness is pivotal for AI in science. Under-confident predictions may lead to misguided conclusions or improper actions. Some approaches [45, 27] directly utilize the entropy observed in the output tokens of the LLMs to gauge the confidence. However, these methods encounter a challenge in our study of ICF whereby the entropy of LLM’s output tokens does not consistently reflect confidence of prediction at each time step. This discrepancy arises due to the non-linear transformation undertaken by the multi-layer

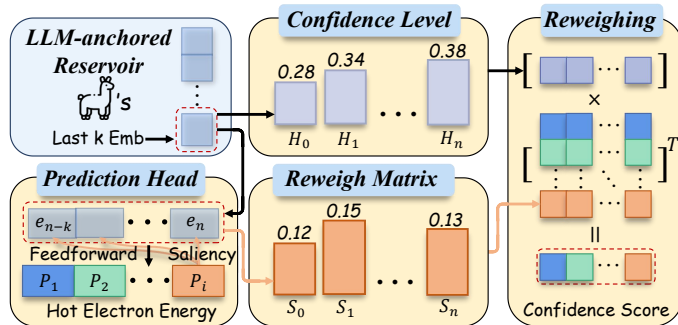


Figure 4: **Pipeline of Confidence Scanner.** We re-calibrate token confidence to align with the energy-prediction head.

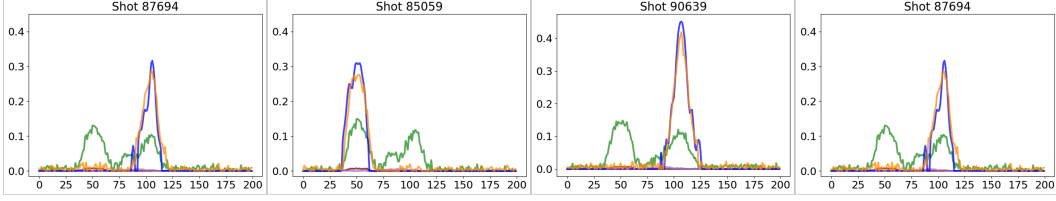


Figure 5: Qualitative results of **hot electron prediction**. We plot **Ground Truth** and the predictions of **Ours**, **Time-LLM**, **LSTM** and **Autoformer**. Y and X axes denote energy and time steps respectively.

perception within the prediction head, which alters the embedding of token counterparts, thereby distorting the relation between tokens and their corresponding confidence estimations.

To this end, we propose *Confidence Scanner* that incorporates a confidence reweighing mechanism to assess the confidence level of each prediction systematically. Concretely, our approach re-calibrates the allocation of confidence across tokens to implicitly reflect their actual influence on predictions. As shown in Fig. 4, we extract the embedding  $E_k = \{e_{n-k}, \dots, e_n\}$  for the last layer of LLM, which specifically analyze the embedding of the last  $k$  tokens. The confidence level  $H$  is then formulated as:

$$H = [h(e_{n-k}), \dots, h(e_n)], \quad (2)$$

where  $h(\cdot)$  map the embedding to word probabilities, which are subsequently used to calculate the entropy. Furthermore, we derive a reweigh matrix  $S$  from the task prediction head  $H_{task}(\cdot)$  by performing a forward process to predict hot-electron energy by  $P = H_{task}(E_k)$ . The matrix  $S$  is then obtained through saliency, reflecting the contribution to the  $i$ -length of predictions:

$$S = \left[ \sigma \left( \frac{\partial P_0}{\partial E_k} \right), \dots, \sigma \left( \frac{\partial P_i}{\partial E_k} \right) \right], \quad (3)$$

where the  $\sigma$  is the softmax function to normalize the saliency scale. Finally, entropy  $H$  is combined with reweigh matrix  $S$  to produce the confidence score  $C = -H \times S$  for the hot electron energy predictions. Through our design, we align the entropy derived from LLM embeddings with the hot electron energy forecasting. This alignment allows us to directly obtain a confidence level that can serve as a trustworthiness indicator for our system. We provide empirical evidence in Fig. 6.

### 3 Empirical Findings

#### 3.1 Main Results

**Dataset.** We develop a new benchmark, FUSION4AI, to support AI research in ICF. This benchmark consists of 40,000 LPI samples containing 100 shot sequences with 400 time steps/shot. Each shot is documented with key parameters such as target size, laser intensity, and energy of hot electrons (see §2.1). The dataset has been systematically divided into 80/10/10 for train/val/test splits respectively. We will release this dataset upon acceptance to advance research for the fusion reaction.

**Baselines.** We choose a classic physical Particle-In-Cell (PIC) simulation method [13], a number of classic AI models (*i.e.*, LSTM [25], Autoformer [86]), reservoir computing models (*i.e.*, HoGRC [43], RCRK [17], NGRC [20]), and concurrent time-series LLM-based models (*i.e.*, GPT4TS [94] and Time-LLM [31]) as baseline models for performance comparison on proposed FUSION4AI dataset.

**Experimental Setup.** Our experiments are trained with 100 epochs and a batch size of 5, which is adequate to achieve convergence based on our empirical findings. In addition, we utilize a fixed learning rate of 0.0004 and the Adam optimizer [36]. A loss function defined by the cumulative absolute error across each time-steps  $f_{\text{loss}}(Y, G) = \sum_{n=1}^{\text{pred\_len}} |y_n - g_n|$  is used, where  $Y$  and  $G$  represent the sequences of predictions and ground truths, respectively,  $y_n$  and  $g_n$  denote the values at the  $n$ -th time-step, and  $\text{pred\_len}$  is the length of prediction. For all other counterpart methods, we follow the original experimental setting and training configurations to reproduce the results.

**Metric.** We employ cumulative absolute error (CAE) as our primary metric. The sole distinction in its implementation involves nullifying values that are less than 0.03 of the predicted value. In addition, we incorporate two supplementary metrics: top-1 and top-5 MAE, which represent mean absolute error focusing exclusively on the top one percent or five percent errors, respectively, thereby highlighting the performance where the highest errors are observed.

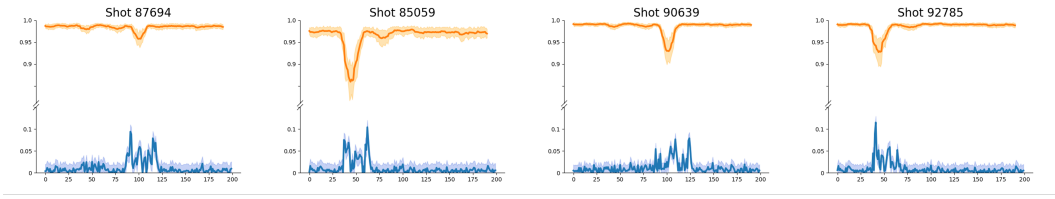


Figure 6: Visualization of **confidence score** and **prediction error**. Samples correspond to Fig. 5.

### Performance Comparison.

The primary challenge in forecasting for ICF lies in developing a robust yet efficient predictive model. Table 1 empirically demonstrates the effectiveness of our system in predicting output energy in ICF, showcasing a significant advantage over all other baseline methods across all metrics. Specifically, our

approach with Llama-3 surpasses PIC simulation model [13] by **0.98** in terms of CAE. Additionally, compared to classic AI methods, our approach outperforms LSTM [25] and Autoformer [86] by **3.92** and **3.89**, respectively. Our margins in CAE over three other reservoir computing methods, HoGRC [43], RCRK [17], NGRC [20], are **2.30**, **2.41**, and **2.38**, respectively. Moreover, our method outperforms concurrent LLM-based approaches GPT4TS [94] and Time-LLM [31] by **1.44** and **1.58** on CAE, respectively, while maintaining comparable speed. Detailed analysis is supplemented in §S2.

These results underscore the efficacy and efficiency of our LLM-based solution in predicting hot electron dynamics in ICF. By extending LLM’s successful adaptability to the new and exciting domain of fusion energy, our empirical findings represent just the beginning of the innovative opportunities presented by applying LLM algorithms to challenging subjects in scientific exploration.

We further present qualitative results in Fig. 5, aligning with our quantitative findings that our method surpasses all comparative baselines in predictive accuracy. Additionally, Fig. 6 illustrates the confidence scores associated with our predictions. The visualization elucidates a clear correlation between predictive error and confidence scores, indicating high confidence corresponding to low errors and conversely. Notably, our approach consistently demonstrates a heightened level of confidence, particularly in forecasting peak values across the temporal sequence, a critical phase in ICF.

### 3.2 Diagnostic Experiment

This section ablates FUSION-LLM’s systemic design on val split of FUSION4AI. All experiments use the Llama 3 8B variant. **Appendix §S2 has more experimental results.**

**Key Component Analysis.** We first investigate the two principal modules of FUSION-LLM, specifically, Fusion-Specific Prompt and Signal-Digesting Channels. We construct a baseline model with generic dummy prompts which only provide broad, non-specific instructions regarding fusion, and a rudimentary encoder composed of a single linear layer. As shown in Table 2a, the baseline model achieves 3.57 CAE. Upon applying Fusion-Specific Prompt to the baseline, we observe significant improvements for CAE from 3.57 to **2.59**. Furthermore, after incorporating Signal-Digesting Channels into the baseline model, we achieve significant gains of **1.56** CAE. Finally, by integrating both core techniques, our FUSION-LLM delivers the best performance of **1.19** CAE. These findings affirm that the proposed Fusion-Specific Prompt and Signal-Digesting Channels operate synergistically, and validate the effectiveness of our comprehensive model design.

**Fusion-Specific Prompt.** We next study the impact of our Fusion-Specific Prompt by contrasting it with a constructed baseline. This baseline incorporates Signal-Digesting Channels and employs generic prompts that provide broad, nonspecific instructions unrelated to the process of fusion. As shown in Table 2b, the baseline yields a performance measure of 2.01 in terms of CAE. Upon substituting the generic prompt with one that integrates discipline-specific information, including

Table 1: **Quantitative results** on FUSION4AI test split for hot electron energy predictions (see §3.1 for details). Refer to the metrics section for details of CAE, top-1 and top-5 MAE.

Method	CAE↓	top-1 MAE↓	top-5 MAE↓
PIC Simulation [13]	2.88	0.20	0.13
LSTM [25]	5.82 $\pm$ 0.06	0.35 $\pm$ 0.01	0.35 $\pm$ 0.01
Autoformer [86]	5.79 $\pm$ 0.04	0.35 $\pm$ 0.01	0.34 $\pm$ 0.01
HoGRC [43]	4.20 $\pm$ 0.79	0.25 $\pm$ 0.05	0.22 $\pm$ 0.02
RCRK [17]	4.31 $\pm$ 0.46	0.28 $\pm$ 0.04	0.22 $\pm$ 0.01
NGRC [20]	4.28 $\pm$ 0.68	0.27 $\pm$ 0.04	0.23 $\pm$ 0.02
GPT4TS [94]	3.34 $\pm$ 0.58	0.18 $\pm$ 0.05	0.14 $\pm$ 0.04
Time-LLM [31]	3.48 $\pm$ 0.72	0.18 $\pm$ 0.05	0.15 $\pm$ 0.05
<b>FUSION-LLM (Llama-2-7B)</b>	2.15 $\pm$ 0.26	<b>0.14</b> $\pm$ 0.01	0.12 $\pm$ 0.01
<b>FUSION-LLM (Llama-3-8B)</b>	<b>1.90</b> $\pm$ 0.33	<b>0.14</b> $\pm$ 0.01	<b>0.11</b> $\pm$ 0.01

Table 2: A set of **ablative studies**. The experiments are evaluated on val split.

Algorithm Component	CAE↓	# of samples	Ours	HoGRC [43]	NGRC [20]	Time-LLM [31]
BASELINE	3.57	80	1.19	3.80	3.73	3.60
+ Fusion-Specific Prompt	2.59	60	1.73	3.87	3.84	3.69
+ Signal-Digesting Channels	2.01	40	2.56	4.01	4.08	3.94
<b>Ours (both)</b>	1.19	20	3.47	4.35	4.19	4.10

(a) Key Component Analysis

(d) Different # of Samples

Prompt Type	CAE↓	# of epochs	Ours	HoGRC [43]	NGRC [20]	Time-LLM [31]
BASELINE	2.01	100	1.19	3.80	3.73	3.60
+ Discipline-related Prompt	1.46	50	1.19	3.99	3.83	3.60
+ Input Statistics	1.58	20	1.56	4.12	4.35	4.01
<b>Ours (both)</b>	1.19	10	2.79	5.23	5.50	4.52

(b) Fusion-Specific Prompt

(e) Different # of Epochs

Algorithm Component	CAE↓	Head Dimension	# Params	CAE↓	top-1 MAE↓	top-5 MAE↓
BASELINE	2.59	256	102.4 K	1.23	0.14	0.12
+ Temporal Encoder	2.47	128	51.2 K	1.19	0.14	0.11
+ Spatial Encoder	1.41	64	25.6 K	1.34	0.14	0.11
<b>Ours (both)</b>	1.19	32	12.8 K	1.57	0.14	0.13

(c) Signal-Digesting Channels

(f) Different Head Dimension

background knowledge, task instructions, *etc*, there is an observable enhancement in performance, achieving an improvement of **0.55** in CAE over the baseline. Additionally, a further analysis involving the integration of input statistics, containing the maximum and minimum values, *etc*, of the input time series, demonstrates superior performance, outperforming the baseline by **0.43** in CAE. The most notable enhancement is recorded when employing our Fusion-Specific Prompt, which amalgamates both the discipline-related information and input statistics, culminating in a peak performance of **1.19** CAE. This outcome highlights the essential function of the Fusion-Specific Prompt within our approach, significantly impacting the performance of the overall model.

**Signal-Digesting Channels.** We then examine the influence of Signal-Digesting Channels in Table 2c. For the baseline, we use a basic approach comprising solely a single linear layer. Under this setting, the baseline model achieves 2.59 in terms of CAE. Integration of either the Temporal Encoder or the Spatial Encoder independently results in performance improvements of **0.12** and **1.18** above the baseline respectively. Conversely, the integration of both Encoders in SDC substantially surpasses all alternative counterparts, achieving a CAE of **1.19**. These results substantiate the hypothesis that the proposed Signal-Digesting Channels augment the capability of our approach to more accurately interpret input time series data.

**Reservoir and LLM Comparison.** To thoroughly explore the training effectiveness of our methodology under conditions of limited sample availability, we perform a comparative analysis using a variable number of training samples with two concurrent reservoir methods [43, 20] and one LLM-based method [31] in Table 2d using CAE. The empirical findings demonstrate that our approach consistently outperforms all competing strategies across various sample configurations. Notably, this superior performance and training effectiveness are evident even with as few as 20 samples. Such robust efficacy is critical in scientific AI applications, where datasets are often constrained in size.

In addition, we study the training efficiency of our approach in contrast to the above strong baselines [43, 20, 31] in Table 2e, across various training epochs. The experimental outcomes illustrate that our approach not only outperforms its counterparts but also demonstrates superior efficiency. Specifically, our method is capable of achieving comparable or superior performance in a significantly reduced training duration. For instance, our model requires only 10 epochs to achieve better performance than other methods that require 100 epochs. This enhanced efficiency in training is particularly significant, as it demonstrates the potential of our approach to deliver robust performance swiftly, thereby facilitating more expedient research in practical scenarios.

**Prediction Head Dimension.** Lastly, we conduct additional experiments to evaluate the impact of varying dimensions in the prediction head. As shown in Table 2f, our approach demonstrates an enhancement in CAE, reducing from 1.57 to **1.34**, concomitant upon augmenting the head dimension from 32 to 64. This improvement continues, culminating in a CAE of **1.19** at a head dimension of 128, where it stabilizes, indicating this as the optimal head dimension for balancing effectiveness and parameter-efficiency. We therefore select the dimension of 128 as the default setting.

## 4 Related Work and Discussion

**AI for Science.** AI is increasingly acknowledged as a critical instrument and recently led trending of significant scientific discovery [32, 40, 55, 5]. The trajectory of AI in scientific research commenced with different elementary data analysis methods (*e.g.*, Rule-based [11, 60], Bayesian [19], Analogy [24, 30, 76], Evolutionary [35, 16], Connectionism [83, 40], *etc*) and has evolved into the advanced foundation models [23, 81, 15, 18, 10]. This development is underscored by considerable progress in AI recently, particularly the emergence of sophisticated constructs such as LLMs [2, 78, 75, 95], which have fundamentally altered our approach to scientific challenges. By incorporating expansive knowledge bases, AI is indispensable for deciphering vast and varied scientific data.

The uniqueness of our work lies in the challenging nature of accessing ICF data, given the difficulty in observing LPI, which renders conventional AI tools less effective in this crucial area of physics. Building on the success of LLMs, this study harnesses their extensive knowledge base to unlock robust predictive capabilities for physical phenomena. Our empirical findings validate our methodological approach, positioning our work as pioneering and innovative. This not only demonstrates the applicability of LLMs in the scientific domain but also fosters a dynamic interplay between AI and scientific exploration. We showcase the potential of our LLM-based solution to make meaningful contributions in addressing complex scientific challenges, thus advancing both AI and science.

**Plasma Physics for Fusion.** In the realm of plasma physics, particularly in ICF, efficient and symmetric driving of a target is imperative. Specifically, LPI represents significant impediments due to the complex dynamics of phenomena in fusion. For instance, Stimulated Raman and Brillouin Scattering (SRS and SBS) can cause the reflection of laser beams [37]. Moreover, Cross-Beam Energy Transfer [28] may adversely influence the symmetry of implosion. A critical issue particularly in direct drive scenarios is the preheating caused by hot electrons produced via SRS and Two-Plasmon Decay, which potentially increases the shell entropy and diminishes the implosion efficiency [68, 21, 14, 54]. Conversely, these hot electrons might contribute positively by depositing their energy in the compressed shell, thereby enhancing the ignition shock and aiding ignition processes such as those observed in shock ignition, a novel high-gain strategy [9, 53]. Understanding the dynamics of LPI and establishing predictive models for hot electron generation in direct drive configurations are crucial. In response to these issues and challenges, extensive physical experimentation and simulations [68, 21, 14, 54, 9, 53] are necessary, which are both costly and time-consuming.

To address the above challenges, our AI-based approach emerges as a potential alternative. By reformulating LLMs with a simple yet effective pipeline, our model can effectively engage in such ICF tasks as Computational Reservoir to encapsulate domain-specific knowledge and generalize within the domain. This capability potentially allows LLMs to guide ICF design, circumventing the need for extensive and expensive experimental setups and simulations. Empirical evidence indicates that the incorporation of LLMs had promising to revolutionize the predictive modeling in plasma physics by providing quick, cost-effective insights that are grounded in generalizable knowledge.

**Reservoir Computing.** The ICF data exhibits a time-series nature, where laser intensity influences the target, correlating with the volume of hot electron energy emission. Traditional machine learning approaches [72, 7, 3, 84, 61, 62, 33] for time-series data typically involve dynamically transforming temporal inputs into a high-dimensional state space through nonlinear mappings. Revolutionary advancements in the field, such as echo state networks [29, 47] and liquid state machines [49, 92], have introduced the concept of Reservoir Computing (RC). RC presents an innovative framework [51, 63, 20, 48] characterized by a static “reservoir”. This reservoir is pre-trained, reducing the computational expenses associated with training only the readout parameters, rather than the entire network. This feature makes RC advantageous for applications involving temporal data [48, 82]. In this paradigm, the input signals are transformed non-linearly into a dynamic time-series system’s state space, from which outputs are linearly extracted [74].

In contrast to traditional reservoirs (*e.g.*, RNN-based [20, 48]) that often struggle with processing highly dynamic temporal data, and contemporary time-series Large Language Models (LLMs) [79, 4, 31, 94] that employ massive parameters but focus solely on temporal sequences, often neglecting the vast knowledge embedded within LLMs, we propose a re-imagining of LLMs within the RC paradigm. This innovative integration not only leverages extensive domain-specific knowledge and adept handling of temporal data but also reduces the need for extensive meta-parameter tuning by maintaining most parameters as static during training. Consequently, our approach emerges as a compelling alternative, effectively addressing the challenges posed by both traditional RNN-based reservoirs and modern time-series LLMs, showcasing superior capability in handling intricate and large-scale temporal patterns.

## 5 Conclusion

Fusion energy stands as a pivotal pathway toward advancing human civilization to a Type I status on the Kardashev scale [34]. The key to realizing this potential lies in mastering Inertial Confinement Fusion, where understanding laser-plasma instabilities is paramount. To address this challenge, we present FUSION-LLM, a groundbreaking framework merging LLMs with reservoir computing. Our approach not only provides a cost-effective solution but also emerges as a top-tier contender in forecasting hot electron dynamics, offering invaluable insights for plasma scientists in refining ICF designs. Beyond its immediate impact on ICF, employing LLMs for scientific exploration holds promise for cross-domain applications, potentially catalyzing advancements in AI-driven scientific endeavors.

## References

- [1] Abu-Shawareb, H., Acree, R., Adams, P., Adams, J., Addis, B., Aden, R., Adrian, P., Afeyan, B., Aggleton, M., Aghaian, L., et al.: Achievement of target gain larger than unity in an inertial fusion experiment. *Physical Review Letters* **132**(6), 065102 (2024)
- [2] Achiam, J., Adler, S., Agarwal, S., Ahmad, L., Akkaya, I., Aleman, F.L., Almeida, D., Altenschmidt, J., Altman, S., Anadkat, S., et al.: Gpt-4 technical report. arXiv preprint arXiv:2303.08774 (2023)
- [3] Ahmed, N.K., Atiya, A.F., Gayar, N.E., El-Shishiny, H.: An empirical comparison of machine learning models for time series forecasting. *Econometric Reviews* **29**(5-6), 594–621 (2010)
- [4] AI, M.: Llama 3 model card. Meta (2024), [https://github.com/meta-llama/llama3/blob/main/MODEL\\_CARD.md](https://github.com/meta-llama/llama3/blob/main/MODEL_CARD.md)
- [5] Ali, S., Ravi, P., Williams, R., DiPaola, D., Breazeal, C.: Constructing dreams using generative ai. In: AAAI (2024)
- [6] Anthropic: The claude 3 model family: Opus, sonnet, haiku. Anthropic (2024), [https://www-cdn.anthropic.com/de8ba9b01c9ab7cbabf5c33b80b7bbc618857627/Model\\_Card\\_Claude\\_3.pdf](https://www-cdn.anthropic.com/de8ba9b01c9ab7cbabf5c33b80b7bbc618857627/Model_Card_Claude_3.pdf)
- [7] Arel, I., Rose, D.C., Karnowski, T.P.: Deep machine learning-a new frontier in artificial intelligence research [research frontier]. *IEEE Computational Intelligence Magazine* **5**(4), 13–18 (2010)
- [8] Betti, R., Hurricane, O.: Inertial-confinement fusion with lasers. *Nature Physics* **12**, 435–448 (2016)
- [9] Betti, R., Zhou, C.D., Anderson, K.S., Perkins, L.J., Theobald, W., Solodov, A.A.: Shock ignition of thermonuclear fuel with high areal density. *Physical Review Letters* **98**, 155001 (2007)
- [10] Bommasani, R., Hudson, D.A., Adeli, E., Altman, R., Arora, S., von Arx, S., Bernstein, M.S., Bohg, J., Bosselut, A., Brunskill, E., et al.: On the opportunities and risks of foundation models. arXiv preprint arXiv:2108.07258 (2021)
- [11] Breiman, L.: Random forests. *Machine Learning* **45**, 5–32 (2001)

- [12] Brown, T., Mann, B., Ryder, N., Subbiah, M., Kaplan, J.D., Dhariwal, P., Neelakantan, A., Shyam, P., Sastry, G., Askell, A., et al.: Language models are few-shot learners. In: *NeurIPS* (2020)
- [13] Cao, S., Patel, D., Lees, A., Stoeckl, C., Rosenberg, M., Gopalaswamy, V., Wen, H., Huang, H., Shvydky, A., Betti, R., et al.: Predicting hot electron generation in inertial confinement fusion with particle-in-cell simulations. *Physical Review E* **106**(5), 055214 (2022)
- [14] Craxton, R.S., Anderson, K.S., Boehly, T.R., Goncharov, V.N., Harding, D.R., Knauer, J.P., McCrory, R.L., McKenty, P.W., Meyerhofer, D.D., Myatt, J.F., Schmitt, A.J., Sethian, J.D., Short, R.W., Skupsky, S., Theobald, W., Kruer, W.L., Tanaka, K., Betti, R., Collins, T.J.B., Delettrez, J.A., Hu, S.X., Marozas, J.A., Maximov, A.V., Michel, D.T., Radha, P.B., Regan, S.P., Sangster, T.C., Seka, W., Solodov, A.A., Soures, J.M., Stoeckl, C., Zuegel, J.D.: Direct-drive inertial confinement fusion: A review. *Physics of Plasmas* **22**(11), 110501 (2015)
- [15] Devlin, J., Chang, M.W., Lee, K., Toutanova, K.: Bert: Pre-training of deep bidirectional transformers for language understanding. *arXiv preprint arXiv:1810.04805* (2018)
- [16] Dietterich, T.G.: Ensemble methods in machine learning. In: *International Workshop on Multiple Classifier Systems*. pp. 1–15. Springer (2000)
- [17] Dong, J., Ohana, R., Rafayelyan, M., Krzakala, F.: Reservoir computing meets recurrent kernels and structured transforms. In: *NeurIPS* (2020)
- [18] Dosovitskiy, A., Beyer, L., Kolesnikov, A., Weissenborn, D., Zhai, X., Unterthiner, T., Dehghani, M., Minderer, M., Heigold, G., Gelly, S., Uszkoreit, J., Houlsby, N.: An image is worth 16x16 words: Transformers for image recognition at scale. In: *ICLR* (2021)
- [19] Frank, E., Trigg, L., Holmes, G., Witten, I.H.: Naive bayes for regression. *Machine Learning* **41**, 5–25 (2000)
- [20] Gauthier, D.J., Bollt, E., Griffith, A., Barbosa, W.A.: Next generation reservoir computing. *Nature Communications* **12**(1), 1–8 (2021)
- [21] Goncharov, V.N., Sangster, T.C., Radha, P.B., Betti, R., Boehly, T.R., Collins, T.J.B., Craxton, R.S., Delettrez, J.A., Epstein, R., Glebov, V.Y., Hu, S.X., Igumenshchev, I.V., Knauer, J.P., Loucks, S.J., Marozas, J.A., Marshall, F.J., McCrory, R.L., McKenty, P.W., Meyerhofer, D.D., Regan, S.P., Seka, W., Skupsky, S., Smalyuk, V.A., Soures, J.M., Stoeckl, C., Shvarts, D., Frenje, J.A., Petrasso, R.D., Li, C.K., Seguin, F., Manheimer, W., Colombant, D.G.: Performance of direct-drive cryogenic targets on omega. *Physics of Plasmas* **15**(5), 056310 (2008)
- [22] Gopalaswamy, V., Williams, C., Betti, R., Patel, D., Knauer, J., Lees, A., Cao, D., Campbell, E., Farmakis, P., Ejaz, R., et al.: Demonstration of a hydrodynamically equivalent burning plasma in direct-drive inertial confinement fusion. *Nature Physics* pp. 1–7 (2024)
- [23] He, K., Zhang, X., Ren, S., Sun, J.: Deep residual learning for image recognition. In: *CVPR* (2016)
- [24] Hearst, M.A., Dumais, S.T., Osuna, E., Platt, J., Scholkopf, B.: Support vector machines. *IEEE Intelligent Systems and their Applications* **13**(4), 18–28 (1998)
- [25] Hochreiter, S., Schmidhuber, J.: Long short-term memory. *Neural Computation* **9**(8), 1735–1780 (1997)
- [26] Huang, W., Abbeel, P., Pathak, D., Mordatch, I.: Language models as zero-shot planners: Extracting actionable knowledge for embodied agents. In: *ICML* (2022)
- [27] Huang, Y., Song, J., Wang, Z., Chen, H., Ma, L.: Look before you leap: An exploratory study of uncertainty measurement for large language models. *arXiv preprint arXiv:2307.10236* (2023)
- [28] Igumenshchev, I.V., Edgell, D.H., Goncharov, V.N., Delettrez, J.A., Maximov, A.V., Myatt, J.F., Seka, W., Shvydky, A., Skupsky, S., Stoeckl, C.: Crossed-beam energy transfer in implosion experiments on omega. *Physics of Plasmas* **17**(12), 122708 (2010)

- [29] Jaeger, H.: Echo state network. *scholarpedia* **2**(9), 2330 (2007)
- [30] Jain, A.K., Murty, M.N., Flynn, P.J.: Data clustering: a review. *ACM Computing Surveys* **31**(3), 264–323 (1999)
- [31] Jin, M., Wang, S., Ma, L., Chu, Z., Zhang, J.Y., Shi, X., Chen, P.Y., Liang, Y., Li, Y.F., Pan, S., et al.: Time-llm: Time series forecasting by reprogramming large language models. In: *ICLR* (2023)
- [32] Jumper, J., Evans, R., Pritzel, A., Green, T., Figurnov, M., Ronneberger, O., Tunyasuvunakool, K., Bates, R., Židek, A., Potapenko, A., et al.: Highly accurate protein structure prediction with alphafold. *Nature* **596**(7873), 583–589 (2021)
- [33] Kadous, M.W.: Learning comprehensible descriptions of multivariate time series. In: *ICML* (1999)
- [34] Kardashev, N.S.: Transmission of Information by Extraterrestrial Civilizations. *Soviet Astronomy* **8**, 217 (1964)
- [35] Kennedy, J., Eberhart, R.: Particle swarm optimization. In: *ICNN* (1995)
- [36] Kingma, D.P., Ba, J.: Adam: A method for stochastic optimization. In: *ICLR* (2015)
- [37] Kirkwood, R.K., Montgomery, D.S., Afeyan, B.B., Moody, J.D., MacGowan, B.J., Joshi, C., Wharton, K.B., Glenzer, S.H., Williams, E.A., Young, P.E., Kruer, W.L., Estabrook, K.G., Berger, R.L.: Observation of the nonlinear saturation of langmuir waves driven by ponderomotive force in a large scale plasma. *Physical Review Letters* **83**, 2965–2968 (1999)
- [38] Klimo, O., Weber, S., Tikhonchuk, V.T., Limpouch, J.: Particle-in-cell simulations of laser–plasma interaction for the shock ignition scenario. *Plasma Physics and Controlled Fusion* **52**(5), 055013 (2010)
- [39] Kojima, T., Gu, S.S., Reid, M., Matsuo, Y., Iwasawa, Y.: Large language models are zero-shot reasoners. In: *NeurIPS* (2022)
- [40] LeCun, Y., Bengio, Y., Hinton, G.: Deep learning. *Nature* **521**(7553), 436–444 (2015)
- [41] Li, C., Wong, C., Zhang, S., Usuyama, N., Liu, H., Yang, J., Naumann, T., Poon, H., Gao, J.: Llava-med: Training a large language-and-vision assistant for biomedicine in one day. In: *NeurIPS* (2023)
- [42] Li, J., Zhang, S., Krauland, C.M., Wen, H., Beg, F.N., Ren, C., Wei, M.S.: Pump depletion and hot-electron generation in long-density-scale-length plasma with shock-ignition high-intensity laser. *Physical Review E* **101**, 033206 (2020)
- [43] Li, X., Zhu, Q., Zhao, C., Duan, X., Zhao, B., Zhang, X., Ma, H., Sun, J., Lin, W.: Higher-order granger reservoir computing: simultaneously achieving scalable complex structures inference and accurate dynamics prediction. *Nature Communications* **15**(1), 2506 (2024)
- [44] Lin, B., Zhu, Y., Chen, Z., Liang, X., Liu, J., Liang, X.: ADAPT: vision-language navigation with modality-aligned action prompts. In: *CVPR* (2022)
- [45] Lin, Z., Trivedi, S., Sun, J.: Generating with confidence: Uncertainty quantification for black-box large language models. *arXiv preprint arXiv:2305.19187* (2023)
- [46] Liu, H., Li, C., Wu, Q., Lee, Y.J.: Visual instruction tuning. In: *NeurIPS* (2023)
- [47] Lukoševičius, M.: A practical guide to applying echo state networks. In: *Neural Networks: Tricks of the Trade: Second Edition*, pp. 659–686. Springer (2012)
- [48] Lukoševičius, M., Jaeger, H.: Reservoir computing approaches to recurrent neural network training. *Computer Science Review* **3**(3), 127–149 (2009)
- [49] Maass, W.: Liquid state machines: motivation, theory, and applications. *Computability in context: computation and logic in the real world* pp. 275–296 (2011)

- [50] Moor, M., Banerjee, O., Abad, Z.S.H., Krumholz, H.M., Leskovec, J., Topol, E.J., Rajpurkar, P.: Foundation models for generalist medical artificial intelligence. *Nature* **616**(7956), 259–265 (2023)
- [51] Nakajima, K., Fischer, I.: *Reservoir computing*. Springer (2021)
- [52] Paszke, A., Gross, S., Massa, F., Lerer, A., Bradbury, J., Chanan, G., Killeen, T., Lin, Z., Gimelshein, N., Antiga, L., et al.: Pytorch: An imperative style, high-performance deep learning library. In: *NeurIPS* (2019)
- [53] Perkins, L.J., Betti, R., LaFortune, K.N., Williams, W.H.: Shock ignition: A new approach to high gain inertial confinement fusion on the national ignition facility. *Physical Review Letters* **103**, 045004 (2009)
- [54] Radha, P., Hohenberger, M., Edgell, D., Marozas, J., Marshall, F., Michel, D., Rosenberg, M., Seka, W., Shvydky, A., Boehly, T., et al.: Direct drive: Simulations and results from the national ignition facility. *Physics of Plasmas* **23**(5), 056305 (2016)
- [55] Reichstein, M., Camps-Valls, G., Stevens, B., Jung, M., Denzler, J., Carvalhais, N., Prabhat, f.: Deep learning and process understanding for data-driven earth system science. *Nature* **566**(7743), 195–204 (2019)
- [56] Rezayi, S., Liu, Z., Wu, Z., Dhakal, C., Ge, B., Zhen, C., Liu, T., Li, S.: Agribert: Knowledge-infused agricultural language models for matching food and nutrition. In: *IJCAI* (2022)
- [57] Riconda, C., Weber, S., Tikhonchuk, V., Héron, A.: Kinetic simulations of stimulated raman backscattering and related processes for the shock-ignition approach to inertial confinement fusion. *Physics of Plasmas* **18**(9), 092701 (2011)
- [58] Rosenberg, M., Solodov, A., Myatt, J., Seka, W., Michel, P., Hohenberger, M., Short, R., Epstein, R., Regan, S., Campbell, E., et al.: Origins and scaling of hot-electron preheat in ignition-scale direct-drive inertial confinement fusion experiments. *Physical Review Letters* **120**(5), 055001 (2018)
- [59] Rosenberg, M., Solodov, A., Seka, W., Follett, R., Myatt, J., Maximov, A., Ren, C., Cao, S., Michel, P., Hohenberger, M., et al.: Stimulated raman scattering mechanisms and scaling behavior in planar direct-drive experiments at the national ignition facility. *Physics of Plasmas* **27**(4) (2020)
- [60] Safavian, S.R., Landgrebe, D.: A survey of decision tree classifier methodology. *IEEE Transactions on Systems, Man, and Cybernetics* **21**(3), 660–674 (1991)
- [61] Samuel, A.L.: Some studies in machine learning using the game of checkers. *IBM Journal of Research and Development* **3**(3), 210–229 (1959)
- [62] Sapankevych, N.I., Sankar, R.: Time series prediction using support vector machines: a survey. *IEEE Computational Intelligence Magazine* **4**(2), 24–38 (2009)
- [63] Schrauwen, B., Verstraeten, D., Van Campenhout, J.: An overview of reservoir computing: theory, applications and implementations. In: *European Symposium on Artificial Neural Networks*. pp. 471–482 (2007)
- [64] Sclar, M., Choi, Y., Tsvetkov, Y., Suhr, A.: Quantifying language models’ sensitivity to spurious features in prompt design or: How I learned to start worrying about prompt formatting. *arXiv preprint arXiv:2310.11324* (2023)
- [65] Sclar, M., Choi, Y., Tsvetkov, Y., Suhr, A.: Quantifying language models’ sensitivity to spurious features in prompt design or: How i learned to start worrying about prompt formatting. In: *ICLR* (2024)
- [66] Shang, W.L., Betti, R., Hu, S.X., Woo, K., Hao, L., Ren, C., Christopherson, A.R., Bose, A., Theobald, W.: Electron shock ignition of inertial fusion targets. *Physical Review Letters* **119**, 195001 (2017)

- [67] Singhal, K., Azizi, S., Tu, T., Mahdavi, S.S., Wei, J., Chung, H.W., Scales, N., Tanwani, A., Cole-Lewis, H., Pfohl, S., et al.: Large language models encode clinical knowledge. *Nature* **620**(7972), 172–180 (2023)
- [68] Smalyuk, V.A., Shvarts, D., Betti, R., Delettrez, J.A., Edgell, D.H., Glebov, V.Y., Goncharov, V.N., McCrory, R.L., Meyerhofer, D.D., Radha, P.B., Regan, S.P., Sangster, T.C., Seka, W., Skupsky, S., Stoeckl, C., Yaakobi, B., Frenje, J.A., Li, C.K., Petrasso, R.D., Séguin, F.H.: Role of hot-electron preheating in the compression of direct-drive imploding targets with cryogenic  $d_2$  ablaters. *Physical Review Letters* **100**, 185005 (2008)
- [69] Smalyuk, V., Shvarts, D., Betti, R., Delettrez, J., Edgell, D., Glebov, V.Y., Goncharov, V., McCrory, R., Meyerhofer, D., Radha, P., et al.: Role of hot-electron preheating in the compression of direct-drive imploding targets with cryogenic  $d_2$  ablaters. *Physical Review Letters* **100**(18), 185005 (2008)
- [70] Solodov, A., Rosenberg, M., Seka, W., Myatt, J., Hohenberger, M., Epstein, R., Stoeckl, C., Short, R., Regan, S., Michel, P., et al.: Hot-electron generation at direct-drive ignition-relevant plasma conditions at the national ignition facility. *Physics of Plasmas* **27**(5) (2020)
- [71] Stoeckl, C., Bahr, R., Yaakobi, B., Seka, W., Regan, S., Craxton, R., Delettrez, J., Short, R., Myatt, J., Maximov, A., et al.: Multibeam effects on fast-electron generation from two-plasmon-decay instability. *Physical Review Letters* **90**(23), 235002 (2003)
- [72] Sutton, R.S.: Learning to predict by the methods of temporal differences. *Machine Learning* **3**, 9–44 (1988)
- [73] Szot, A., Clegg, A., Undersander, E., Wijmans, E., Zhao, Y., Turner, J.M., Maestre, N.D., Mukadam, M., Chaplot, D.S., Maksymets, O., Gokaslan, A., Vondruš, V., Dharur, S., Meier, F., Galuba, W., Chang, A.X., Kira, Z., Koltun, V., Malik, J., Savva, M., Batra, D.: Habitat 2.0: Training home assistants to rearrange their habitat. In: *NeurIPS* (2021)
- [74] Tanaka, G., Yamane, T., Héroux, J.B., Nakane, R., Kanazawa, N., Takeda, S., Numata, H., Nakano, D., Hirose, A.: Recent advances in physical reservoir computing: A review. *Neural Networks* **115**, 100–123 (2019)
- [75] Team, G., Anil, R., Borgeaud, S., Wu, Y., Alayrac, J.B., Yu, J., Soricut, R., Schalkwyk, J., Dai, A.M., Hauth, A., et al.: Gemini: a family of highly capable multimodal models. *arXiv preprint arXiv:2312.11805* (2023)
- [76] Tenenbaum, J.B., Silva, V.d., Langford, J.C.: A global geometric framework for nonlinear dimensionality reduction. *Science* **290**(5500), 2319–2323 (2000)
- [77] Thirunavukarasu, A.J., Ting, D.S.J., Elangovan, K., Gutierrez, L., Tan, T.F., Ting, D.S.W.: Large language models in medicine. *Nature Medicine* **29**(8), 1930–1940 (2023)
- [78] Touvron, H., Lavril, T., Izacard, G., Martinet, X., Lachaux, M.A., Lacroix, T., Rozière, B., Goyal, N., Hambro, E., Azhar, F., et al.: Llama: Open and efficient foundation language models. *arXiv preprint arXiv:2302.13971* (2023)
- [79] Touvron, H., Martin, L., Stone, K., Albert, P., Almahairi, A., Babaei, Y., Bashlykov, N., Batra, S., Bhargava, P., Bhosale, S., Bikel, D., Blecher, L., Canton-Ferrer, C., Chen, M., Cucurull, G., Esiobu, D., Fernandes, J., Fu, J., Fu, W., Fuller, B., Gao, C., Goswami, V., Goyal, N., Hartshorn, A., Hosseini, S., Hou, R., Inan, H., Kardas, M., Kerkez, V., Khabsa, M., Kloumann, I., Korenev, A., Koura, P.S., Lachaux, M., Lavril, T., Lee, J., Liskovich, D., Lu, Y., Mao, Y., Martinet, X., Mihaylov, T., Mishra, P., Molybog, I., Nie, Y., Poulton, A., Reizenstein, J., Rungta, R., Saladi, K., Schelten, A., Silva, R., Smith, E.M., Subramanian, R., Tan, X.E., Tang, B., Taylor, R., Williams, A., Kuan, J.X., Xu, P., Yan, Z., Zarov, I., Zhang, Y., Fan, A., Kambadur, M., Narang, S., Rodriguez, A., Stojnic, R., Edunov, S., Scialom, T.: Llama 2: Open foundation and fine-tuned chat models. *CoRR* (2023)
- [80] Tzachor, A., Devare, M., Richards, C., Pypers, P., Ghosh, A., Koo, J., Johal, S., King, B.: Large language models and agricultural extension services. *Nature Food* **4**(11), 941–948 (2023)

- [81] Vaswani, A., Shazeer, N., Parmar, N., Uszkoreit, J., Jones, L., Gomez, A.N., Kaiser, Ł., Polosukhin, I.: Attention is all you need. In: NeurIPS (2017)
- [82] Verstraeten, D., Schrauwen, B., d’Haene, M., Stroobandt, D.: An experimental unification of reservoir computing methods. *Neural Networks* **20**(3), 391–403 (2007)
- [83] Weisberg, S.: *Applied linear regression*, vol. 528. John Wiley & Sons (2005)
- [84] Williams, C.K., Rasmussen, C.E.: *Gaussian processes for machine learning*. MIT press Cambridge, MA (2006)
- [85] Woo, G., Liu, C., Kumar, A., Xiong, C., Savarese, S., Sahoo, D.: Unified training of universal time series forecasting transformers. arXiv preprint arXiv:2402.02592 (2024)
- [86] Wu, H., Xu, J., Wang, J., Long, M.: Autoformer: Decomposition transformers with Auto-Correlation for long-term series forecasting. In: NeurIPS (2021)
- [87] Yaakobi, B., Stoeckl, C., Seka, W., Delettrez, J., Sangster, T., Meyerhofer, D.: Measurement of preheat due to fast electrons in laser implosions of cryogenic deuterium targets. *Physics of Plasmas* **12**(6) (2005)
- [88] Yaakobi, B., Stoeckl, C., Boehly, T., Meyerhofer, D., Seka, W.: Measurement of preheat due to fast electrons in laser implosions. *Physics of Plasmas* **7**(9), 3714–3720 (2000)
- [89] Yan, R., Li, J., Ren, C.: Intermittent laser-plasma interactions and hot electron generation in shock ignition. *Physics of Plasmas* **21**(6), 062705 (2014)
- [90] Yao, S., Zhao, J., Yu, D., Du, N., Shafran, I., Narasimhan, K.R., Cao, Y.: React: Synergizing reasoning and acting in language models. In: ICLR (2023)
- [91] Zhang, A., Yang, J., Luo, Y., Fan, S.: Forecasting the progression of human civilization on the kardashev scale through 2060 with a machine learning approach. *Scientific Reports* **13**(1), 11305 (2023)
- [92] Zhang, Y., Li, P., Jin, Y., Choe, Y.: A digital liquid state machine with biologically inspired learning and its application to speech recognition. *IEEE Transactions on Neural Networks and Learning Systems* **26**(11), 2635–2649 (2015)
- [93] Zheng, L., Chiang, W., Sheng, Y., Zhuang, S., Wu, Z., Zhuang, Y., Lin, Z., Li, Z., Li, D., Xing, E.P., Zhang, H., Gonzalez, J.E., Stoica, I.: Judging llm-as-a-judge with mt-bench and chatbot arena. In: NeurIPS (2023)
- [94] Zhou, T., Niu, P., Sun, L., Jin, R., et al.: One fits all: Power general time series analysis by pretrained lm. In: NeurIPS (2023)
- [95] Zhu, D., Chen, J., Shen, X., Li, X., Elhoseiny, M.: Minigt-4: Enhancing vision-language understanding with advanced large language models. arXiv preprint arXiv:2304.10592 (2023)

## SUMMARY OF THE APPENDIX

This supplementary contains additional experimental results and discussions of our NeurIPS 2024 submission: *Inertial Confinement Fusion Forecasting via LLMs*, organized as follows:

- §S1 provides **Implementation Details**.
- §S2 reports more **Quantitative Results** with **Runtime Analysis**.
- §S3 shows more **Qualitative Results**.
- §S4 analyzes **Failure Case**.
- §S5 conducts **Confidence Analysis**.
- §S6 discusses the **Social Impact & Limitation** of our research.
- §S7 offers **Ethical Guard** of our dataset.
- §S8 claims **Reproducibility** of our approach.
- §S9 supplies **Data License** for the methods we used for comparison.

### S1 Implementation Details

The overall pipeline of FUSION-LLM is shown in Fig. 3. Experiments are conducted on two NVIDIA A100-40GB GPUs. For our approach, we keep all parameters of the LLMs and most of the SDC frozen during the fine-tuning. Only parameters pertaining to the Prediction Head and partial Spatial Encoder are trainable. The codes and dataset shall be publicly released upon paper acceptance.

- FUSION-LLM is built from Llama-2-7B-hf / 3-8B [78, 4] to construct reservoir without tuning.
- *Fusion-specific prompts* structure the textual prompts with three descriptors: context descriptor, task descriptor, and input descriptor. Each descriptor is initialized with specialized tokens for indication (*e.g.*,  $\langle |begin\_of\_text| \rangle$ ,  $\langle |eot\_id| \rangle$ ,  $\langle |start\_header\_id| \rangle$ , *etc*) and input scalars as context descriptions (*e.g.*,  $\langle seq\_len \rangle$ ,  $\langle pred\_len \rangle$ ,  $\langle phase\_plate \rangle$ , *etc*). These prompts are subsequently concatenated and input into the projection layer from LLMs for feature embedding.
- *Signal-digesting channels* are composed of two components, temporal encoder and spatial encoder. The former one, which incorporates 24 Transformer layers and a linear layer, captures temporal features over the input laser signal. This module has been pre-trained on the Large-scale Open Time Series Archive (LOTSAs) dataset [85], which covers nine varied domains and compiles over 27 billion timestamped instances. The spatial decoder first uses a projection block from Llama [78, 4] to encode the context description of the input signal, followed by a leaner transformation. Outputs are fed into a cross-attention layer, where Key and Value are derived from the contextual embedding and query stems from temporal features, to generate the final spatial features. We concatenate the spatial and temporal features before feeding them into a linear layer to produce the final, augmented input signals.
- *Confidence scanner* has been described in §2.2.3 and it has no consumption of parameters. The default number of tokens  $k$  used in confidence calculation is set to 50 in the implementation.
- *Prediction head* consists of two layers: a convolution layer with the kernel size of 32 and stride of 32, followed by batch normalization and GELU activation, connected to LLM, then fed to a linear layer with the input dimension of 128 that produces the final prediction.

### S2 Quantitative Results

This section elaborates on a detailed analysis of quantitative results in Table S1, focusing specifically on in-context learning [12] performance and a runtime assessment of the models under investigation. Initially, we present supplementary in-context learning results obtained directly from various LLMs (*i.e.*, Llama 2 [79], Llama 3 [4], and Claude 3 Opus [6]). These findings indicate that, even without an additional fine-tuning process, the LLMs exhibit substantial proficiency in the in-context learning scheme within the ICF task. For instance, Claude 3 Opus [6] achieves CAE scores of 12.19, 10.67, and 9.46 for the 1-shot, 2-shot, and 3-shot scenarios, respectively. It is amply demonstrated that the vanilla LLM has the ability to make inferences and predictions on empirical scientific data even if it is not fine-tuned at all. This underscores that our approach, leveraging these LLMs, represents a notable advancement, particularly in forecasting the energy dynamics of hot electrons.

Table S1: **Quantitative results** on FUSION4AI test split for hot electron energy forecasting (see §3.1 for details). Train Time refer to training for the designated task, and Infer Time refer to the amount of time used to predict one case. Note that 3-shot experiments could not be performed on Llama series of models due to the limitation of context window.

Method	# Params	Train Time	Infer Time	CAE↓	top-1 MAE↓	top-5 MAE↓
PIC Simulation [13]	-	-	> 10 hrs	2.88	0.20	0.13
LSTM [25]	81.6K	~5 mins	< 1 s	5.82	0.35	0.35
Autoformer [86]	120.4K	~8 mins	< 1 s	5.79	0.35	0.34
GPT4TS [94]	1.5 B	~22 mins	~2 s	3.34	0.18	0.14
Time-LLM [31]	7 B	~20 mins	~3 s	3.48	0.18	0.15
Llama 2 (1-Shot) [79]	7 B	-	~3 s	471.22	15.80	14.92
Llama 2 (2-Shot) [79]	7 B	-	~5 s	30.33	0.95	0.91
Llama 2 (1-Shot) [79]	70 B	-	~7 s	20.63	0.64	0.63
Llama 2 (2-Shot) [79]	70 B	-	~8 s	16.42	0.51	0.50
Llama 3 (1-Shot) [4]	8 B	-	~4 s	583.14	17.70	16.97
Llama 3 (2-Shot) [4]	8 B	-	~6 s	26.66	0.83	0.81
Llama 3 (1-Shot) [4]	70 B	-	~14 s	72.35	1.02	1.15
Llama 3 (2-Shot) [4]	70 B	-	~19 s	13.62	0.40	0.39
Claude 3 Opus (1-Shot) [6]	137 B	-	~12 s	12.19	0.39	0.39
Claude 3 Opus (2-Shot) [6]	137 B	-	~17 s	10.67	0.38	0.37
Claude 3 Opus (3-Shot) [6]	137 B	-	~20 s	9.46	0.37	0.36
RCRK [17]	106K	~2 mins	< 1 s	4.31	0.28	0.22
HoGRC [43]	394K	~4 mins	< 1 s	4.20	0.25	0.22
NGRC [20]	157K	~2 mins	< 1 s	4.28	0.27	0.23
<b>FUSION-LLM (Llama-2)</b>	7B	~30 mins	~3 s	2.15	0.14	0.12
<b>FUSION-LLM (Llama-3)</b>	8B	~30 mins	~4 s	1.90	0.14	0.11

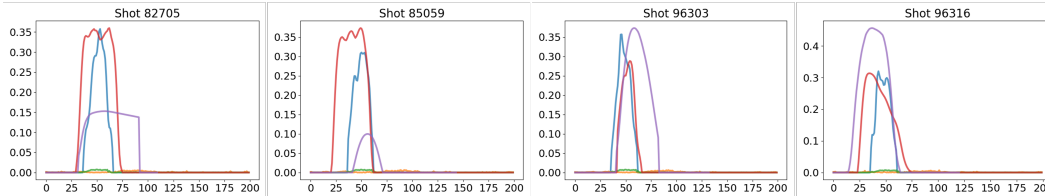


Figure S1: Predictions of **LLMs with In-Context Learning**. We plot **Ground Truth** and the predictions of **Claude 3 Opus (3-shot)** and **Llama 3 70B (2-shot)** with the comparison of trained methods **LSTM** and **Autoformer**. Y and X axes denote energy and time steps.

Furthermore, it is pertinent to emphasize the economic and operational advantages of our computational approach over traditional physical experiments. Specifically, conducting a single ICF experiment typically incurs costs upwards of one million US dollars. Conversely, computational simulations such as a  $150\mu\text{m}$  PIC simulation [13] require extensive computational resources, amounting to the utilization of 19,584 cores of CPU over a period of 10 hours. In stark contrast, our model necessitates significantly less computational time and resources, requiring only 30 minutes on 2 NVIDIA A100 GPUs for training and only 3~4 seconds for inference with much higher predictive accuracy compared to the PIC simulation. This comparison not only underscores the cost-effectiveness of our approach but also its efficiency and practicality in other scientific applications where computational resource constraints are a critical factor.

### S3 More Qualitative Result

This section expands to include more qualitative results that help to understand the capabilities and effectiveness of this model. Initially, we release all visualized prediction results of our model FUSION-LLM on test split of our dataset FUSION4AI in Fig. S2. From these qualitative results, it can be found that our model achieves accurate predictions on all unseen data, especially conforming

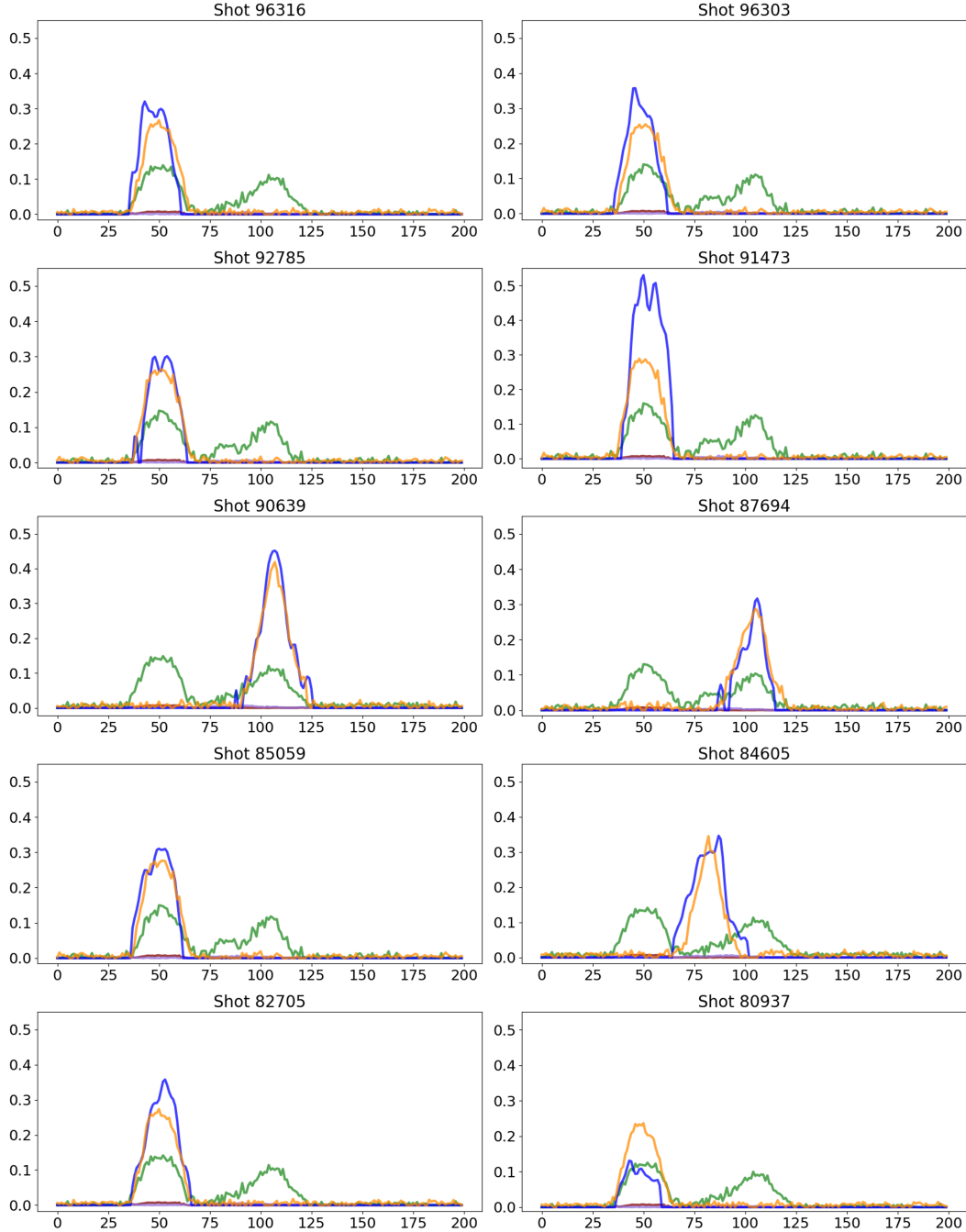


Figure S2: Visualization of **hot electron prediction** in test split. We plot **Ground Truth** and the predictions of **Ours**, **Time-LLM**, **LSTM** and **Autoformer**. Y and X axes denote energy and time steps, respectively.

to the temporal and spatial characteristics of the predicted targets, which is crucial for physicists to apply our model as a tool in the design of real-world ICF shots.

Recall that we describe in §S2, the direct prediction of ICF tasks by vanilla LLM use in-context learning method without fine-tuning on our data is not as good as fine-tuned methods in terms of the quantitative value of metric, but it can in fact predict more meaningful patterns than traditional methods such as LSTM [25] and Autoformer [86]. As illustrated in Figure S1, the LLM without fine-tune can infer approximate predictions with reference to the 1 to 3 examples provided, as compared to

LSTM [25] and Autoformer [86] which can only predict straight lines close to 0 with patterns. This proves that the vanilla LLMs themselves already contain the capability to infer specific empirical scientific data, which is the core reason we chose LLMs as the reservoir of our FUSION-LLM.

## S4 Failure Case Analysis

In this section, we examine a significant outlier with the largest error forecasts generated by the FUSION-LLM on the test split. This particular instance serves as a critical case study for understanding the limitations and challenges faced by our model. Fig. S3 illustrates that the shot markedly deviates from the typical scenarios. Notably, this shot exhibits an exceptionally low peak hot electron energy, registering less than 0.15, whereas the majority of other cases yield values ranging between 0.25 and 0.5 under a comparable input laser profile. This anomaly categorizes this shot as an out-of-distribution (OOD) instance. The limited volume of training data available for FUSION-LLM is a plausible explanation for the model’s diminished performance on this OOD data. In scenarios where training data is sparse, the model’s capability to generalize to new, especially atypical, data points is inherently restricted. Consequently, this case highlights the importance of enhancing the dataset’s diversity and volume for ICF tasks. We hope the community can share more data points to improve and enlarge FUSION4AI dataset (§3.1) together.

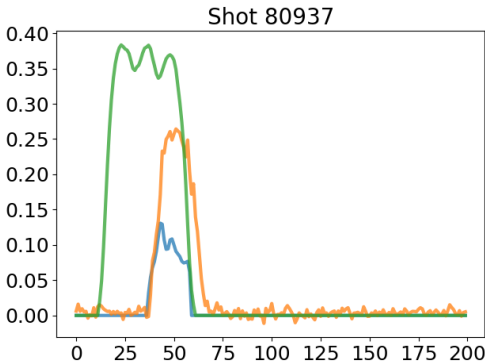


Figure S3: The Qualitative result of Shot 80937. We plot **Input Laser Intensity**, **Ground Truth** and **Prediction**. Y axis denotes laser intensity / hot electron energy, and X axis denotes time step.

## S5 Confidence Analysis

In this section, we provide a comprehensive discussion and analysis of the confidence scores associated with the FUSION-LLM. As elaborated in §2.2.3, our confidence scores offer per-step evaluations, thereby aiding physicists to gain deeper insights into the reliability across various segments of predictions. This functionality is particularly vital for understanding the model’s performance dynamics within specific contexts of its predictive output.

To visually represent this, we have plotted the prediction errors at each time step for the four test sets alongside their respective confidence scores in Fig. S4. The visual analysis reveals that the confidence scores exhibit a discernible decline in the intervals where the model’s predictions incur larger errors compared to other intervals. This observation substantiates the existence of a correlation between the model’s diminished confidence and the occurrence of higher prediction inaccuracies.

Such an analysis underscores the importance of confidence scores as a diagnostic tool, highlighting intervals where the model’s predictions are potentially less reliable. By mapping these confidence scores to the corresponding prediction errors, physicists can identify specific phases within the prediction and temporal sequence where the model’s forecasting should be interpreted with caution. This capability not only enhances the trustworthiness of the FUSION-LLM but also provides critical feedback for further refinement of the model in the future research.

Moreover, the integration of confidence scores into the model’s predictive framework offers a robust mechanism for assessing the model’s performance in real-time applications. By continuously monitoring these scores, physicists can make informed decisions about the reliability of the predictions, ensuring that critical assessments and subsequent actions are based on the most credible forecasting.

## S6 Social Impacts and Limitations

The introduction of FUSION-LLM represents a significant advancement in integrating LLMs with classical reservoir computing paradigms to enhance predictive capabilities in Inertial Confinement Fusion. This novel approach not only meets but exceeds several existing state-of-the-art models in performance benchmarks. From a societal perspective, the implications of FUSION-LLM are

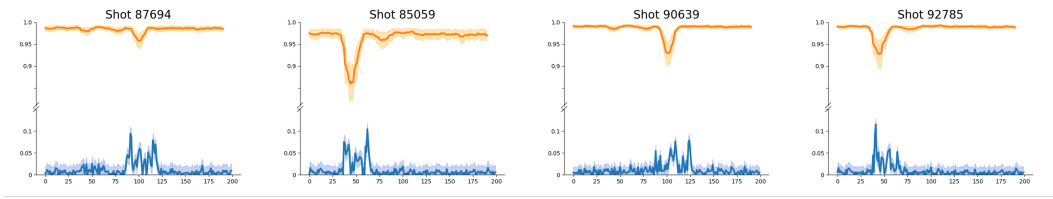


Figure S4: Qualitative results of **confidence score** and **prediction error**.

profoundly beneficial, as our approach provides a valuable tool for advancing our understanding and capabilities in harnessing fusion energy — a potential key to long-term sustainable energy solutions. However, it is imperative to acknowledge and critically assess the potential drawbacks associated with this technology. Similar to other predictive models, FUSION-LLM faces challenges when dealing with out-of-distribution data or scenarios that have not been previously encountered. This limitation underscores the need for ongoing research and refinement, particularly in its application to real-world ICF scenarios where unpredictable behaviors might emerge. Therefore, while the model demonstrates promising applications, its deployment in practical settings must be approached with caution, ensuring continuous evaluation and adaptation to maintain reliability and safety in its predictive assertions.

## S7 Ethical Safeguards

In our paper, which involves a new dataset, we will establish comprehensive ethical safeguards to mitigate potential misuse and ensure responsible utilization, as outlined in the detailed protocols in the final release of models and datasets. These protocols include strict usage guidelines, access restrictions, integration of safety filters, and monitoring mechanisms. We conduct thorough risk assessments to identify potential misuse scenarios, developing tailored mitigation strategies such as robust data governance frameworks. Although not all research may require stringent safeguards, we adhere to best practices, promoting ethical awareness encouraging researchers to consider the broader impacts of their work and maintain detailed documentation for transparency and accountability. These efforts demonstrate our commitment to upholding the highest standards of ethical conduct in scientific inquiry, aiming to safeguard the interests and privacy of all people involved.

## S8 Reproducibility

FUSION-LLM is implemented in PyTorch [52]. Experiments are conducted on two NVIDIA A100-40GB GPUs. To guarantee reproducibility, our full implementation shall be publicly released upon paper acceptance.

## S9 Licenses for existing assets

All the methods we used for comparison are publicly available for academic usage. PIC Simulation is implemented based on the reproducing by `osiris-code/osiris` with AGPL-3.0 license. We use `huggingface/transformers` for the implementations of Autoformer [86], Llama 2 [79] and Llama 3 [4] with Apache-2.0 license and Llama 2/3 Community License Agreement. We used the official repositories `DAMO-DI-ML/NeurIPS2023-One-Fits-All` (GPT4TS [94]), `KimMeen/Time-LLM` [31], `rubenohana/Reservoir-computing-kernels` (RCRK [17]), `CsnowyLstar/HoGRC` [43] and `quantinfo/ng-rc-paper-code` (NGRC [20]) for our comparison experiments, where Time-LLM [31] is licensed under Apache-2.0, HoGRC [43] and NGRC [20] are licensed under MIT, the rest did not mention their licenses.